Electrochemical AFM on Surface Grafted Poly(ferrocenylsilanes)

Mária Péter, Mark A. Hempenius, Rob G. H. Lammertink, Julius G. Vancso*

MESA+ Research Institute, University of Twente, Faculty of Chemical Technology, Department of Materials Science and Technology of Polymers, P.O. Box 217, 7500 AE Enschede, The Netherlands

SUMMARY: Ethylenesulfide and trimethylenesulfide end-functionalized poly(ferrocenyldimethylsilanes) (ES-PFS and TMS-PFS) with different degrees of polymerization were prepared via anionic ring-opening polymerization. Molecular characterization of ES-PFS was carried out by using ^{1}H-NMR, GPC, FTIR, and elemental analysis. Thin films of ES-PFS were prepared by immersing gold(111) substrates into 1.0 mg/ml solutions of the polymers in toluene. The polymeric films were characterized by FTIR, XPS, and contact angle measurements. Thicknesses of the grafted films were measured by SPR. Thicknesses determined by SPR and the theoretically calculated values are in a reasonable agreement. The morphology of the films was studied by tapping mode AFM. The electrochemical behavior of the films was monitored by cyclic voltammetry (CV). CVs show two reversible redox peaks, indicating a stepwise oxidation of the iron atoms in the polymer chains. Scanning Electrochemical Force Microscopy (SEFM) allowed us to study in situ the morphological changes occurring in the film upon electrochemical oxidation or reduction. AFM images indicated that in the oxidized form the chains were stretched due to electrostatic repulsion.

Introduction

Poly(ferrocenyldimethylsilanes) (PFS) exhibit interesting electrochemical and other potentially useful properties owing to their unique structure, which incorporates redox active ferrocene units and Si atoms in the main chain.[1)] The attachment of a thiol end-function to the polymer chain allows one to immobilize PFS onto gold surfaces by the self-assembly technique.[2,3)] This process can be used to modify the surface of an electrode with variable surface concentrations of the electroactive centers and to study the charge transfer through the polymeric layer at the electrode/electrolyte interface. The electrochemical oxidation/reduction of the electroactive centers manifests itself in a conformational change of the polymer coils due to the presence of electrostatic repulsion between the charged electroactive centers. The morphological changes occurring at different potentials can be followed in situ by electrochemical atomic force microscopy (ECAFM).

 CCC 1022-1360/00/$ 17.50+.50/0

Experimental Section

N,N,N',N'-Tetramethylethylenediamine (TMEDA), ferrocene, dichlorodimethylsilane, and *n*-butyllithium were purchased from Aldrich. TMEDA was distilled from sodium prior to use. Dimethylsilylferrocenophane monomer was prepared as described earlier.[4,5] Ethylenesulfide and trimethylenesulfide were purchased from Aldrich, and distilled as hexane solutions using CaH_2 as drying agent prior to use. The polymerization reactions were carried out in tetrahydrofuran (THF), using *n*-buthyllithium as initiator, in a glovebox purged with prepurified nitrogen. After two hours, the living polymers were terminated by adding three equivalents of ethylenesulfide or trimethylenesulfide. The thiolate end groups were protonated by adding a few drops of acid acetic. Thus, ethylenesulfide and trimethylensulfide end-functionalized poly(ferrocenyldimethylsilanes) (PFS), denoted as ES-PFS and TMS-PFS, were obtained. The polymers were precipitated twice from methanol and dried in vacuo.

GPC measurements were carried out in THF using microstyragel columns with pore sizes of 10^6, 10^5, 10^4, and 10^3 Å (Waters) equipped with a dual detection system consisting of a differential refractometer (Waters model 410) and a differential viscometer (Viscotek model H502). The molar masses were referenced to a polystyrene calibration curve. ^{1}H-NMR spectra ($CDCl_3$) were recorded on a 300 MHz Varian Inova Nuclear Magnetic Resonance Spectrometer. Elemental analyses were carried out using a Carlo Erba Elementar Analyzer 1108 for simultaneous CHNS/O determinations.

Fourier Transform Infrared Spectroscopy (FTIR) measurements were done using a Bio-Rad Enhanced Intensity FT-IR 575C Spectrometer. The chamber of the instrument was purged with dry nitrogen. The spectra were taken with a resolution of 4 cm^{-1} (2800 scans) at a scan speed of 5 kHz, and they were baseline corrected at the end. The bulk spectroscopic characterization of ES-PFS and TMS-PFS was undertaken in KBr pellets using a deuterated triglycine sulfate (DTGS) detector. The polymeric layers on gold were characterized by reflection-absorption grazing-angle incidence FTIR spectroscopy (the incidence angle was θ_i = 83°) using a mercury cadmium telluride (MCT) detector cooled with liquid nitrogen. For this purpose the FTIR spectrometer was equipped with a uniflex optical device, which allows a focused infrared beam to reflect at a surface in the horizontal plane. This can be done at any angle by rotating the arms of the uniflex. The background spectra were recorded for $C_{16}D_{33}SH$

self-assembled monolayers on gold substrate. The absorption of CO_2 and sometimes also of water could not be completely avoided when spectra of the polymeric layers were taken.

Evaporated gold substrates (borosilicat glass, 2 nm Cr, 250 nm Au) were purchased from Metallhandel Schröer (Lienen, Germany). Au(111) samples were prepared by annealing the gold substrates in a high purity hydrogen flame for 8 minutes. Round gold (diameter 2.5 cm) substrates were prepared by the evaporation of 5 nm of Cr followed by 200 nm of Au on glass substrates. Prior to use, these substrates were cleaned in piranha solution (mixture of 1:4 of 30% H_2O_2 and concentrated H_2SO_4), then rinsed with MilliQ water and ethanol, and dried in a nitrogen stream. *Caution! Piranha solution is a very strong oxidant, reacts violently with organic materials and should be handled with utmost care!* Thin films of end-functionalized PFS were prepared by immersing gold substrates into 1.0 mg ml^{-1} solutions of the polymers in toluene for at least 24 h to ensure maximum coverage. The samples were subsequently rinsed with toluene and dried in a stream of nitrogen.

Contact angles were measured with a Krüss G10 Contact Angle Measuring Instrument equipped with a CCD camera. Advancing and receding contact angles were determined automatically by the drop shape analysis routine during the growth and shrinkage of the droplet. Contact angles were measured using MilliQ water. X-Ray Photoelectron Spectroscopy (XPS) spectra were obtained on a Quick Scan Kratos XSAM800 (Manchester, UK) instrument using a Mg Kα radiation source (1253.6 eV). The analyzer slit width was set to 6 mm and the input power was 150 W (15 kW/10 mA). Survey scans in a binding energy window of 1100-0 eV were recorded with a pass energy of 100 eV. Spectra were obtained for electron take-off angles of 0° (perpendicular) and 60° (to the normal). Atomic concentrations were determined by the numerical integration of the relative peak areas in the detailed element scans using sensitivity factors given in the literature.[6)]

Scanning Force Microscopy (SFM) measurements were performed with a NanoScope III AFM (Digital Instruments (DI), Santa Barbara, USA) in the tapping mode. The images were taken in air using rectangular Si-cantilevers with a spring constant of 20-54 N/m. Electrochemical Scanning Force Microscopy (ECSFM) experiments were done in contact mode using an electrochemical liquid cell (DI) (volume 50 µl). Triangular SiN_3 cantilevers with a spring constant of 0.32 N/m were utilized. The polymer covered gold was the working electrode, Pt wire reference and counter electrodes were used. The electrolyte used was 0.1 M

$NaClO_4$ in water. Prior to use the electrolyte was deaerated by passing nitrogen trough the solution.

Surface plasmon resonance measurements were performed against 0.1 M $NaClO_4$ in the Kretschmann configuration.[7)] A refractive index of n = 1.687 was assumed for all layers. The refractive index was determined previously by profilometry followed by ellipsometry.

Electrochemical experiments (cyclic voltammetry (CV)) were undertaken using an Autolab PGSTAT10 (ECOCHEMIE, Utrecht, The Netherlands) in a three electrode configuration. Polymer covered gold disk working, $Hg/HgSO_4$ (MSE) reference (+0.61 V_{NHE}) and Pt auxiliary electrodes were used. The electrolyte was 0.1 M $NaClO_4$ in water. The working electrode exposed a surface area of 0.43 cm^2 to the electrolyte. The cell was degassed by passing nitrogen trough the electrolyte for a few minutes. A constant nitrogen overflow was ensured over the electrolyte during the measurements. The cyclic voltammograms were recorded between –0.3 V_{MSE} and 0.3 V_{MSE} at different scan rates.

Results and Discussion

Ethylenesulfide end-functionalized poly(ferrocenylsilanes) (ES-PFS) with degrees of polymerization (DP) 25, 50, 100 and trimethylenesulfide end-functionalized PFS (TMS-PFS) with degree of polymerization 50 were prepared by anionic ring opening polymerization via the reaction schemes 1 and 2.

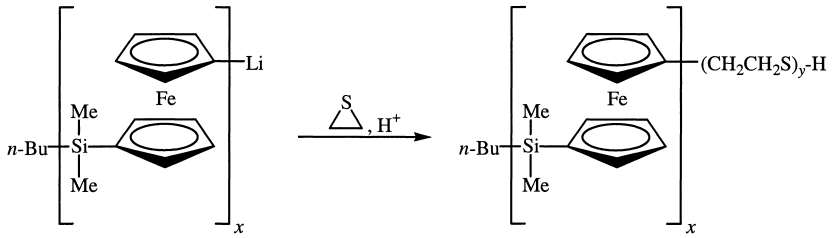

Scheme 1. Synthesis of ethylenesulfide end-grafted poly(ferrocenyldimethylsilane).

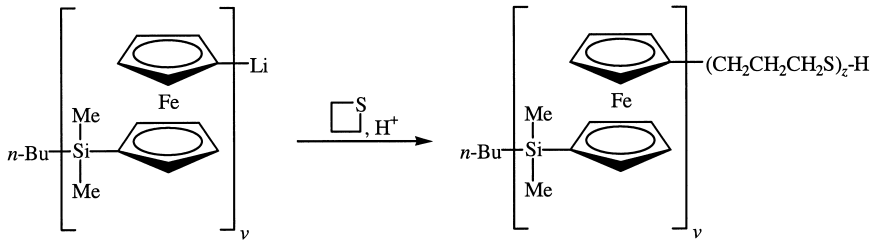

Scheme 2. Synthesis of trimethylenesulfide end-grafted poly(ferrocenyldimethylsilane).

The molecular characteristics of the polymers are summarized in Table 1. The molar masses of the polymers determined by GPC and estimated by end-group analysis using ^{1}H-NMR are in excellent agreement.

Table 1. Molecular characteristics of end-functionalized PFS.

	M_n (g/mol) (GPC)	M_n (g/mol) (^{1}H-NMR)	M_w/M_n (GPC)	DP (observed)	PFS:ES(/TMS) *x*:*y* (*v*:*z*)[a]
ES-PFS25	7750	7740	1.36	32	32:3
ES-PFS50	12500	12320	1.14	50	50:3.75
ES-PFS100	22600	22450	1.13	92	92:2
TMS-PFS50	11300	11200	1.14	46	46:6

[a] see Scheme 1 and Scheme 2 for notations

The peaks found in the ^{1}H-NMR spectra at δ 2.78 (spectra not shown) were assigned to the methylene groups next to the sulfur in the end-group. The signals of the ^{1}H-NMR spectrum at δ 4.22 and 4.00 correspond to the protons (4H) from the cyclopentadienyl rings, while the resonance at δ 0.44 corresponds to the protons (6H) from the methyl groups attached to Si. The absorbances assigned to the C-H vibrations in the ferrocene rings and in the methyl and methylene groups can be found in the FT-IR spectra (Figure 1). The results given by elemental analysis are in good agreement with the theoretically expected values (Table 2).

Table 2. Comparison between the theoretical compositions and those found by elemental analysis for the polymers synthesized.

	Theoretical composition			Experimental		
	C(wt %)	H (wt %)	S (wt %)	C(wt %)	H (wt %)	S (wt %)
ES-PFS25	59.21	5.86	1.28	59.16	6.05	1.07
ES-PFS50	59.26	5.85	0.95	59.17	5.93	1.47
ES-PFS100	59.45	5.81	0.29	59.61	6.12	0.53
TMS-PFS50	59.19	5.93	1.68	59.94	6.02	1.53

The thin polymeric films were characterized by FT-IR, XPS and contact angle measurements. In Figure 1 the overlaid FT-IR spectra for the ES-PFS50 film on gold and in KBr pellet in the high and low energy region are shown. The observed bands can be easily identified based on the structure of the adsorbates.[8] In the high energy region (Figure 1a) the $\nu_{C\text{-}H}$ are observed for the ferrocene rings (3087 cm^{-1}) as well as for the methyl groups (2958 cm^{-1}). In the low energy region (Figure 1b) the most prominent peaks are associated with the symmetric deformation of the CH_3 groups in Si-CH_3 silanes (1248 cm^{-1}), the asymmetric ring in-plane vibration for Fc (1182 and 1165 cm^{-1}), the out-of-plane C-H vibration for Fc (1037 cm^{-1}), the CH_3 rocking vibration in Si-CH_3 silanes (896 cm^{-1}), the Si-C streching vibration (864 cm^{-1}), the in-plane C-H stretching in Fc (819 cm^{-1}), and the out-of-plane C-H deformation for Fc (799 and 768 cm^{-1}).

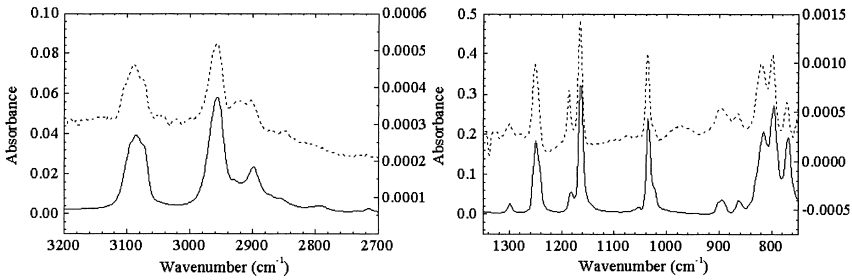

(a) (b)

Figure 1. FTIR spectra for ES-PFS50 in bulk (in KBr) overlaid with the FTIR spectra of ES-PFS50 thin film on gold; (a) high energy region; (b) low energy region.

XPS spectra exhibits peaks associated with C 1s, Fe 2p (from the Fc ring), Si 2s (from the polymer backbone), and S 2p (from the end-function). Atomic concentrations determined by

the integration of the relative peak areas from XPS measurements are shown in Table 3. The ratio Si/Fe almost equals unity, which agrees well with the theoretical composition (Si/Fe = 1). The atomic concentration of S decreases with increasing take-off angle, indicating that the S is located very close to the substrate surface.

Table 3. XPS analysis of the surface grafted polymeric monolayers on gold.

Element		ES-PFS25		ES-PFS50		ES-PFS100		TMS-PFS50	
	Take-off angle	0°	60°	0°	60°	0°	60°	0°	60°
C1s		82.26	87.26	83.68	84.96	85.57	86.99	80.32	84.84
Si2p		8.03	5.6	7.07	6.48	6.6	6.16	8.7	6.98
Fe2p		7.81	6.04	6.92	7.1	6.76	5.98	8.39	6.62
S2p		1.88	1.09	2.31	1.44	1.05	0.86	2.57	1.54

Contact angles with water were measured to determine the wetting properties of the films. Advancing contact angles were found to be *ca.* 96° and receding contact angles *ca.* 75° for all layers, indicating hydrophobic surfaces.

Tapping mode height AFM images (Figure 2) recorded for the ES-PFS layers exhibit a globular surface structure, superimposed on the atomically smooth triangular terraces which are characteristic for the bare Au(111) substrate.[3)] Figure 2 shows an increase in globule size with increasing molar mass of the grafted chains. The underlying triangular terraces of bare Au(111) still can be seen in the AFM images.

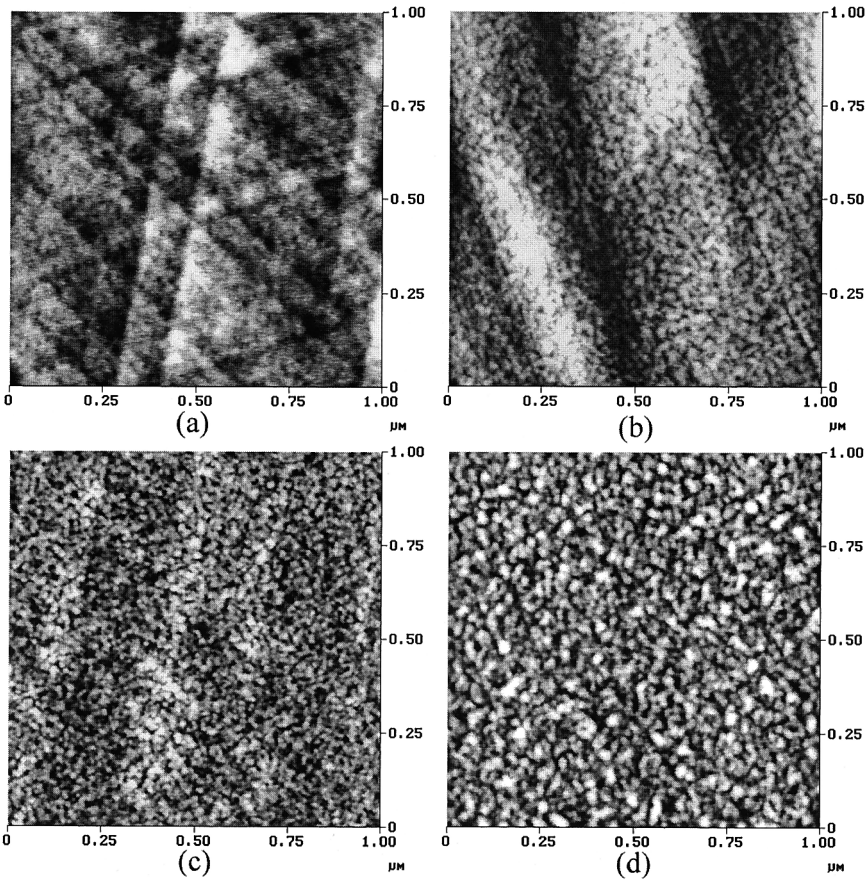

Figure 2. Tapping mode height AFM images recorded for (a) ES-PFS25, (b) ES-PFS50, (c) ES-PFS100, and (d) TMS-PFS50 layers on Au(111) (z range is 10 nm for all images).

Cyclic voltammograms (CVs) recorded for the electroactive polymer layers show two reversible redox peaks, associated with the stepwise, one electron oxidation of the Fe atoms in the ferrocene rings.[9,10] In Figure 3a, a CV recorded on a ES-PFS50 layer, using a scan rate of 10 mV/s is shown. Peak currents plotted against the scan rates show linear behavior, which indicates that the electrochemical answer is due to the adsorbate oxidation/reduction (Figure 3b). The detailed interpretation of the redox mechanism requires further studies.

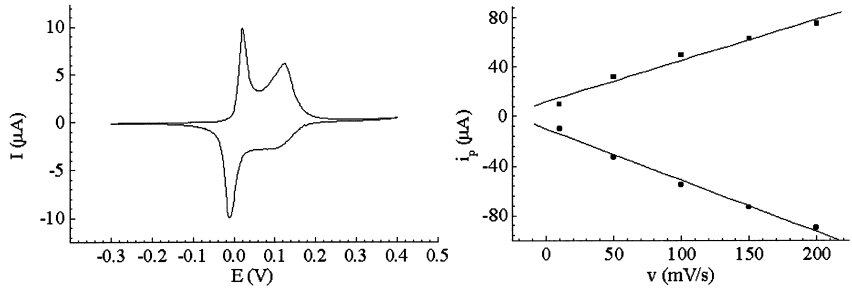

(a) (b)

Figure 3. (a) CV for ES-PFS50 on gold at v = 10 mV/s; (b) linear dependence of peak currents versus scan rates (the upper line is for the oxidation, the lower one is for the reduction process).

The surface coverages of ferrocene sites (Γ_{Fc}) for all layers were determined according to equation 1, where Q_{Fc} is the charge passed for the oxidation/reduction of ferrocene sites,

$$\Gamma_{Fc} = \frac{Q_{Fc}}{nFA} \qquad (1)$$

n is the number of electrons involved in the electron transfer process (n = 1), F is the Faraday constant, and A is the geometric surface area of the electrode. The charge passed in the redox reaction was determined by integrating the areas under the redox peaks. The number of grafted chains per unit area (Γ) was calculated by dividing Γ_{Fc} by the degree of polymerization. Γ is related to the mean distance between attachment points (s), by $\Gamma = 1/s^2$. The unperturbed radius of gyration (R_g) of ES-PFS is almost equal to s, thus the coverage is moderate with chains attached to the surface forming a 'brush' structure. The thickness of a brush in good solvents is given as[11)]

$$L = \frac{Nl^{5/3}}{s} = \Gamma^{1/2} R_F^{5/3} \qquad (2)$$

where L is the thickness, n is the degree of polymerization, l is the effective segment length, and R_F is the Flory-radius ($R_F = \alpha R_g$, where α is the intramolecular expansion factor). The thickness of a 'dry' layer is given by[12)]

$$L_0 \cong l^3 N\Gamma . \qquad (3)$$

For the TMS-PFS layer Rg < s, thus according to the theory we are dealing with a low coverage of polymeric chains. The layer thickness roughly equals the unperturbed radius of gyration in this case. The layer thicknesses were measured by SPR against a 0.1 M $NaClO_4$

electrolyte. The experimentally determined data, as well as the calculated values are shown in Table 4.

Table 4. Coverage and thickness data for the end-grafted PFS layers on gold.

	Γ (chain/nm^2)	s	R_g (nm)	L_0[a] (nm)	L[b] (nm)	L[c] (nm)
ES-PFS25	0.375	1.63	1.48	3.14	9.31	4.94
ES-PFS50	0.274	1.91	1.85	3.60	12.5	6.43
ES-PFS100	0.159	2.51	2.50	3.84	17.4	7.75
TMS-PFS50	0.131	2.77	1.75	1.54	7.91	1.63

[a]calculated thickness of a dry layer

[b]calculated thickness in good solvent

[c]thickness measured by SPR against 0.1 M $NaClO_4$ electrolyte

Upon oxidation of surface grafted PFS, electrostatic repulsion occurs between the Fc^+ centers. As a consequence, it can be anticipated that the polymer coils will stretch. An ECAFM study was undertaken to study this possible conformational change in situ as a function of the applied potential. The CV obtained by cycling the potential between –0.2 and 0.4 V can be seen in Figure 4a. In Figure 4b is shown the temporary current versus time graph, generated as the triangular signal is applied to the working electrode. As the potential is cycled, a morphology change occurs (Figure 4c). Flat regions in the image correspond to potential values close to the reduction potential.

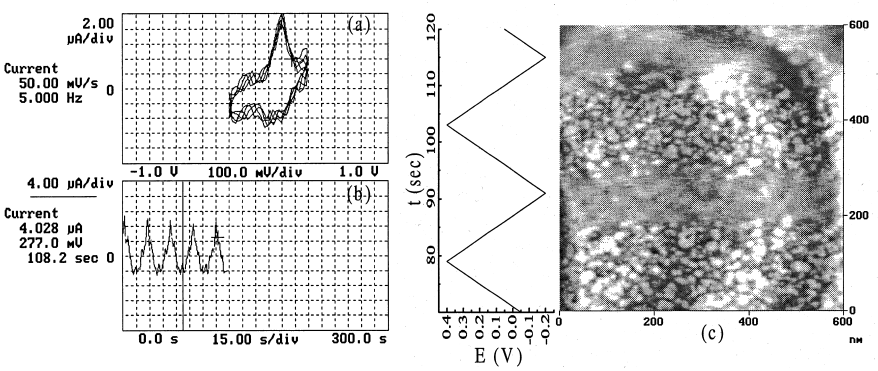

Figure 4. ECAFM experiment on ES-PFS50 layers, recorded at v = 50 mV/s.

The observed change in morphology is reversible as it can be seen in Figure 5.

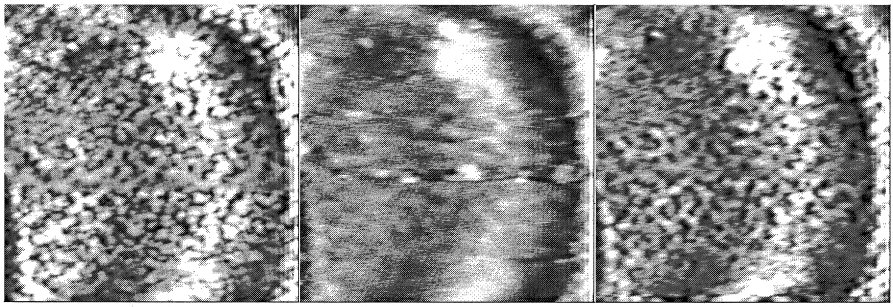

(a) (b) (c)

Figure 5. ECAFM images obtained for ES-PFS50 layers on gold at different potentials (scan size is 600×600 nm^2, z range is 5 nm); (a) E = +110 mV; (b) E = -160 mV; (c) E = +100 mV.

Figure 5a shows an AFM height image recorded at a constant potential of +110 mV, while at –160 mV all chains are expected to be reduced and conformationally more close to a random coil, the surface appears to be almost flat. If the potential is cycled again and held near the oxidation potential the features become higher again (Figure 5c).

Conclusions

ES-PFS layers on gold were prepared by the self-assembly technique. The different characterization techniques indicate that a brush structure is formed on the surfaces with a moderate coverage. TMS-PFS forms a layer with low coverage. Thicknesses determined by SPR and the theoretically calculated values are in a reasonable agreement. Cyclic voltammograms show two reversible redox peaks, indicating a stepwise oxidation of the polymer chains. The ECAFM study revealed that reversible morphology changes occur depending on the potential applied to the electrode. In the oxidized form the chains were stretched due to electrostatic repulsion, as indicated by AFM images.

Acknowledgement

The authors would like to thank to Mr. Clemens Padberg for the GPC measurements. Dr. Toby Jenkins is acknowledged for the SPR measurements. We are grateful for the financial support by the University of Twente.

References

1. I. Manners, *Can. J. Chem.* **76**, 371 (1998)
2. R. G. Nuzzo, D. L. Allara, *J. Am. Chem. Soc.* **105**, 4481 (1983)
3. M. Peter, R. G. H. Lammertink, M. A. Hempenius, M. v. Os, M. W. J. Beulen, D. N. Reinhoudt, W. Knoll, G. J. Vancso, *Chem. Commun.* , 359 (1999)
4. A. B. Fischer, J. B. Kinney, R. H. Staley, M. S. Wringhton, *J. Am. Chem. Soc.* **101**, 6501 (1979)
5. Y. Ni, R. Rulkens, I. Manners, *J. Am. Chem. Soc.* **118**, 4102 (1996).
6. D. Briggs and M. P. Seah, in: *Practical Surface Analysis*, John Wiley & Sons, New York, 1986
7. E. Kretschmann, *Z. Phys.* **241**, 313 (1971)
8. G. Socrates, in: *Infrared Characteristic Group Frequencies. Tables and Charts*, John Wiley & Sons Ltd., Chichester, 1994
9. M. T. Nguyen, A. F. Diaz, V. V. Dement'ev, K. Pannell, *Chem. Mater.* **5**, 1389 (1993)
10. D. Foucher, R. Ziembinski, R. Petersen, J. Pudelski, M. Edwards, Y. Ni, J. Massey, C. R. Jaeger, G. J. Vancso, I. Manners, *Macromolecules* **27**, 3992 (1994)
11. J. N. Israelachvili, in: *Intermolecular and Surface Forces*, Academic Press, London, 1991
12. L. Léger, E. Raphaël, H. Hervet, *Advances in Polymer Science* **138**, 185 (1999)